

# Phase transitions in unstable cancer cell populations

R.V. Solé<sup>1,2,a</sup>

<sup>1</sup> ICREA-Complex Systems Lab, Universitat Pompeu Fabra, Dr Aiguader 80, 08003 Barcelona, Spain

<sup>2</sup> Santa Fe Institute, 1399 Hyde Park Road, New Mexico 87501, USA

Received 22 April 2003

Published online 22 September 2003 – © EDP Sciences, Società Italiana di Fisica, Springer-Verlag 2003

**Abstract.** The dynamics of cancer evolution is studied by means of a simple quasispecies model involving cells displaying high levels of genetic instability. Both continuous, mean-field and discrete, bit-string models are analysed. The string model is simulated on a single-peak landscape. It is shown that a phase transition exists at high levels of genetic instability, thus separating two phases of slow and rapid growth. The results suggest that, under a conserved level of genetic instability the cancer cell population will be close to the threshold level. Implications for therapy are outlined.

**PACS.** 87.10.+e Biological physics: General theory and mathematical aspects – 87.23.Kg Dynamics of evolution – 87.23.-n Ecology and evolution – 89.75.Fb Structures and organization in complex systems

## 1 Introduction

Cancer is the result of a system's breakdown that arises in a cell society when a single cell (due to a mutation or set of mutations) starts to display uncontrolled growth [1]. The cooperation that maintains the integrity of a multicellular organism is thus disrupted. Further changes in the population generated by such abnormal cell can lead to malignant tumor growth, eventually killing the host. From an evolutionary point of view, tumor progression is a microevolution process in which tumors must overcome selection barriers imposed by the organism. The emergence and evolution of tumors involve a number of phenomena that are well known in physics, from pattern formation to phase transitions. In this context, suitable theoretical methods from statistical physics can help to gain insight into cancer biology. Related areas, such as immunology [2] and virus dynamics [3–6] have already revealed the power of physics in exploring complex phenomena within molecular cell biology.

As discussed by Alberts *et al.* [7] a multicellular system is a society or ecosystem whose individual members are cells, reproduced in a collaborative way and organized into tissues. In this sense, understanding it requires concepts that are well-known in population dynamics, such as birth, death, habitat and the maintenance of population sizes. Under normal conditions, there is no need to worry about selection and mutation: as opposed to the survival of the fittest, the cell society involves cooperation and, when needed, the death of its individual units. Mutations

occur all the time but sophisticated mechanisms are employed in detecting them and either repairing the damage or triggering the death of the cell displaying mutations [8]. Abnormal cells can be identified from within (*i.e.* through molecular signaling mechanisms operating inside the damaged cell) or by means of interactions with other cells. The later mechanism involves immune responses.

Selection barriers (such as the attack from the immune system or physical barriers of different types) can be overcome by a tumor provided that the diversity of mutant cells is high enough to generate a successful strain. High mutation rates are thus a way to escape from the host responses and it is actually known that most human cancers are *genetically unstable* [1,9–13]. Genetic instability results from mutations in genes that are implicated in DNA repair or in maintaining the integrity of chromosomes. As a result, mutations accumulate at very high rates. RNA viruses are actually a good example of replicating systems involving mutation and it was early shown that such systems involve an *error threshold*: beyond a critical mutation rate, a phase transition occurs towards a random replication phase [15–19]. At the subcritical, low-mutation phase, the population is able to maintain hereditary information and a heterogeneous distribution of molecules is observed: the so-called quasispecies. At the supercritical phase, populations experience random drift through sequence space and no genetic information can be maintained. The nature of such transition has been well established in terms of a mapping between replication dynamics and spin lattice [20–23] and field models [24].

---

<sup>a</sup> e-mail: ricard.sole@upf.edu

An important implication of the previous observation is that the threshold-like character of the phase transition allows to conjecture that non-viable virus populations might be obtained by slightly increasing the mutation rate beyond criticality. This has been done *in vitro* [25] and *in vivo* therapies are in progress. A similar scenario has been suggested within the context of cancer [10,12]. Since cancer also displays some common traits with RNA viruses it has been suggested that unstable cancer populations might also display threshold levels of mutation parallel to those observed in viral populations [26]. If true, strategies based on targeting unstable cancer cells and increasing their mutation rate would successfully inhibit tumor progression.

In a recent study, it has been shown that a bifurcation from slow-growth to rapid growth exists in a continuous (mean-field) model of cancer evolution [26] involving three basic cell populations. In this paper we further explore this result by extending it to a population model involving  $N$  cell types by means of both mean field and bit-string approaches. A phase transition (and thus a sharp qualitative change in population dynamics) is shown to exist and several statistical features are analysed.

## 2 Mean field quasispecies model

The starting point for a model of molecular replicators involving errors is the general Eigen-Schuster quasispecies model, defined by the following set of equations:

$$\frac{dx_i}{dt} = \sum_{j=1}^n x_j f_j Q_{ji} - \langle f \rangle x_i \quad (1)$$

where  $\mathbf{x} = x_1, \dots, x_n$ , and  $x_i$  indicates the fraction of the population associated to the  $i$ th mutant genome (here  $i = 1, \dots, n$ , where  $n$  is very large) so that populations are restricted to a simplex:  $\sum_j^n x_j = 1$ . Here  $f_j$  is the growth rate of the  $j$ th mutant,  $Q_{ij}$  is the probability of having a mutation  $i \rightarrow j$  and  $\langle f \rangle = \sum_{j=1}^n f_j x_j$  the average fitness.

In its simplest form, we can consider a reduced system of equations defining a population as formed by two basic groups: the master sequence  $x_1$  and the other sequences, which we assume to be grouped into an ‘‘average’’ sequence with population  $x_2$  [14]. Let us also assume that mutations occur from the master to the second compartment but not in the reverse sense. The enormous size of the sequence space makes this assumption a good first approximation. Now we have [14,26]:

$$\frac{dx_1}{dt} = f_1 x_1 Q - x_1 \Phi(x_1, x_2) \quad (2)$$

$$\frac{dx_2}{dt} = f_1 x_1 (1 - Q) + f_2 x_2 - x_2 \Phi(x_1, x_2) \quad (3)$$

where it is assumed that  $f_1 > f_2$ . This oversimplified model allows us to see the error threshold condition under a mean field argument. The fixed points here are located

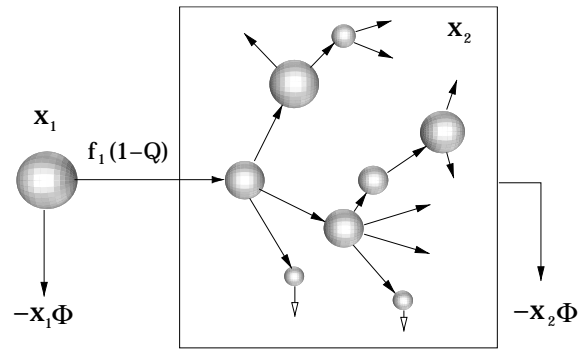


**Fig. 1.** Basic scheme of the population model used in this paper. Here a slow-growth cell population is indicated as  $x_1$ , mutating at a slow rate  $\mu = 1 - Q$ . Some mutations can lead to the emergence of a genetically unstable population (box) involving a very heterogeneous group of cell types, replicating at different rates (here indicated by means of variable radius) and many of them unable to survive (white arrows).

on the line  $x_1^* = 1 - x_2^*$ , with

$$x_2^* = \frac{f_1(1 - Q)}{f_1 - f_2}. \quad (4)$$

It can be shown, by means of standard stability analysis that the state where the master sequence gets extinct (*i.e.*  $(x_1^*, x_2^*) = (0, 1)$ ) will be stable if  $f_1 Q < f_2$ . otherwise, the master sequence is able to survive and Darwinian selection keeps operating. Once the mutation rate exceeds this error threshold, no stable master sequence can persist.

Within the context of unstable cancer cell populations, a two-compartment model can also be defined, as displayed in Figure 1. Here two basic components are considered: a slow-growing, weakly unstable population ( $x_1$ , with a small mutation rate  $\mu = 1 - Q$ ) and a highly heterogeneous set of (unstable) clones ( $\{x_2^i\}$ ), indicated in the right box in Figure 1. These unstable clones would exhibit a high mutation rate  $\mu_u$  (typically  $\mu_u \gg \mu$ ). Assuming that  $x_1 + \sum_i x_2^i = 1$ , and lumping together the unstable compartment so that  $x_2 \equiv \sum_i x_2^i$ , we have a one-dimensional model for the evolution of  $x_1$ :

$$\frac{dx_1}{dt} = f_1 x_1 (\xi_1 - \xi_2 x_1) \quad (5)$$

where  $\xi_1 = Q - f_2/f_1$  and  $\xi_2 = 1 - f_2/f_1$ . The equilibrium points for this system are  $x_1^* = 0$  and  $x_1^* = \xi_1/\xi_2$ . Actually the time-dependent solution is shown to be a sigmoidal function:

$$x_1(t) = \frac{\xi_1}{\xi_2} \left[ 1 + \left( \frac{\xi_1/\xi_2 - x_1(0)}{x_1(0)} \right) \exp(-\xi_1 f_1 t) \right]^{-1} \quad (6)$$

thus showing that the approach to the steady state is a function of the replication and mutation rates.

Based on experimental evidence, it is known that increasing levels of mutation lead to increased rates of cell death. A general relationship can be established between

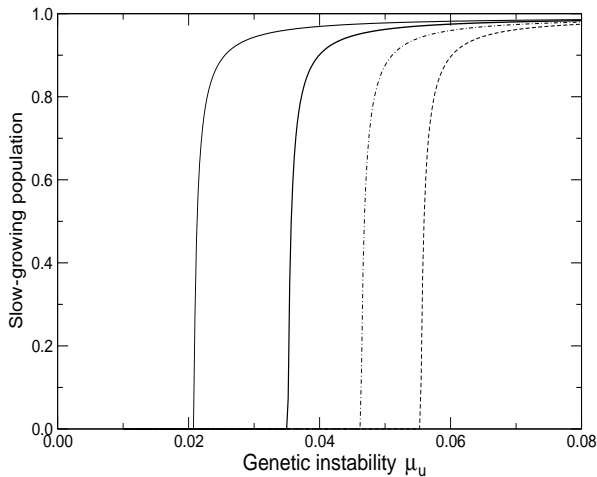


**Fig. 2.** Phase transition in the mean field model of cancer quasispecies. The population size of the slow-growing clone is shown for different values of the genetic instability rate  $\mu_u$ . Here we have  $f_1 = 0.25$ ,  $\mu_u^* = 0.05$  and  $\mu_1 = 0.01$ . Four different values of the selective advantage parameter  $\alpha$  have been used. From left to right,  $\alpha = 1.5, 2.0, 2.5$  and  $3.0$ , respectively.

replication rates as follows:

$$f_2(\mu_u, \alpha) = \alpha f_1 \phi(\mu_u) \quad (7)$$

where  $\alpha > 1$  is a measure of the selective advantage of  $x_2$  over  $x_1$  and  $\phi(\mu_u)$  a decreasing function of the genetic instability level. Here we choose  $\phi(\mu_u) = \exp(-\mu_u/\mu_u^*)$  with  $\mu_u^* = 0.05$ . Using these functional forms, we obtain

$$x_1^*(\mu_u) = \frac{Q - \alpha \phi(\mu_u)}{1 - \alpha \phi(\mu_u)}. \quad (8)$$

The slow-growing clone will only survive provided that  $\mu < \mu_c = Q - \alpha \phi(\mu_u)$ . For our particular choice, this leads to a critical mutation rate

$$\mu_u^c = -\mu_u^* \ln \left( \frac{1 - \mu}{\alpha} \right). \quad (9)$$

In Figure 2 the phase transition behavior predicted by the mean field model is illustrated by showing the equilibrium population of the slow-growing clone  $x_1^*$  against the rate of genetic instability, for different  $\alpha$  values. As predicted by the previous equation (9) a sharp transition occurs from the unstable population phase (where the unstable clones outgrow the  $x_1$  population) and a slow-growth phase, where genetic instability is too high to maintain a finite  $x_2$  population. It is worth mentioning that the critical rate depends on the selective advantage parameter  $\alpha$  and thus a trade-off between replication and mutation rates is at work at the phase transition. In this sense, the critical boundary can be reached in two different ways (either tuning genetic instability levels or replication rates).

The stability of the two fixed points can be determined by looking at the associated Lyapunov function  $\Phi(\mu_u, x_1)$ , defined from

$$\frac{dx_1}{dt} = -\frac{\partial \Phi(x_1, \mu_u)}{\partial x_1} \quad (10)$$

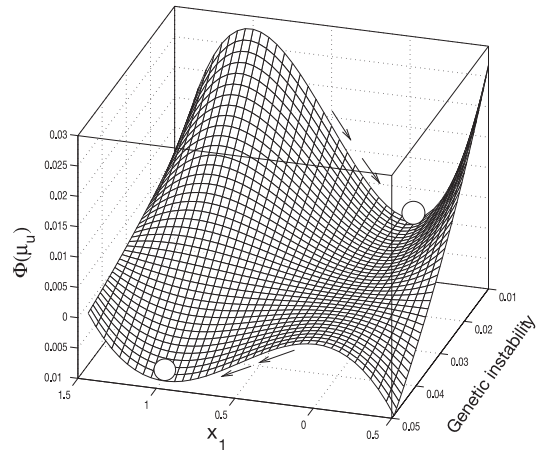


**Fig. 3.** Lyapunov function  $\Phi(\mu_u)$  for the one-dimensional equilibrium state. Here genetic instability acts as the control parameter. A shift occurs from the extinction of the  $x_1$  clone to the dominance of it. The two equilibrium states are indicated as white circles.

*i.e.* from

$$\Phi(x_1, \mu_u) = -f_1 \int_0^{x_1} y_1 (\xi_1 - \xi_2 y_1) dy_1 \quad (11)$$

$$= -f_1 \left[ \frac{1}{2} (Q - \alpha \phi(\mu_u)) x_1^2 - \frac{1}{3} (1 - \alpha \phi(\mu_u)) x_1^3 \right]. \quad (12)$$

The surface  $\Phi(x_1, \mu_u)$  is shown in Figure 3 for  $\mu = 0.01$ ,  $f_1 = 0.25$  and  $\alpha = 2$ . We can appreciate two well-defined minima involving the two (exchanging) equilibrium fixed points.

The previous mean-field approach allows to conjecture that a well-defined transition will be observed close to the error threshold. In order to better understand this phenomenon, we consider in the following section a discrete string model where each cell is described in terms of a small “genome” of a given length  $\nu$ . Mutations are thus explicitly introduced and the statistical behavior of the cell population can be followed in more detail. It also allows to perform comparisons with previous spin-based models of quasispecies dynamics.

### 3 Bit string model: single-peak landscape

A much more informative approach to the cancer quasispecies model is provided by a system composed by  $N$  bit strings. Although these models are again an oversimplified picture of reality, they retain the key features of the underlying evolutionary dynamics [27–29].

Here each string  $S_k$  ( $k = 1, \dots, N$ ) is a small genome of size  $\nu$  *i.e.*

$$S_i = (S_i^1, S_i^2, \dots, S_i^\nu) ; \quad i = 1, 2, \dots, N \quad (13)$$

with  $S_k^i \in \{0,1\}$ . A genome under this description is thus a vertex  $S_k \in \mathcal{H}^\nu$  of a  $\nu$ -dimensional hypercube. Although a real (RNA or DNA) genome is composed by a four-letter alphabet, here we use the approach taken by Leuthäusser, where each bit would represent purines or pyrimidines [20,21].

The sequence  $\xi = (1,1,\dots,1)$  will represent a cell belonging to the  $x_1$ -cell type population. Other strings  $S_k \neq \xi$  will define the unstable compartment, involving  $2^\nu - 1$  different genomes. The possible transitions allowed here are summarized as follows:

$$\xi \xrightarrow{f(\xi)\Gamma} 2\xi \quad (14)$$

$$\xi \xrightarrow{W_{\xi k}} \xi + S_k \quad (15)$$

$$S_i \xrightarrow{f(S_i)\Gamma_u} 2S_i \quad (16)$$

$$S_i \xrightarrow{W_{ik}} S_i + S_k \quad (17)$$

where  $\Gamma \equiv (1-\mu)^\nu$  and  $\Gamma_u \equiv (1-\mu_u)^\nu$ , respectively, where  $\mu$  and  $\mu_u$  will be now mutation rates per bit and round of replication. Accordingly with the mean-field model, the replication rates will be  $f(\xi) = f_1$  and  $f(S_k \neq \xi) = \alpha f(\xi)\phi(\mu_u)$ , respectively. Here we will use a constant replication rate for all strings  $S_k \neq \xi$  and thus for  $\mu_u > \mu_u^c$  we have  $f(\xi) > f(S_k \neq \xi)$  and a single-peaked landscape will be at work, as in the Swetina-Schuster model [14]. For  $\mu_u < \mu_u^c$  the unstable population will dominate on a flat landscape with a ‘‘hole’’ at  $S_k = \xi$ .

The terms  $W_{ij}$  correspond to the probabilities of erroneous replication and are given by:

$$W_{\xi k} = f(\xi)(1-\mu)^{\nu-d_H[\xi,S_k]}\mu^{d_H[\xi,S_k]} \quad (18)$$

$$W_{jk} = f(S_k)(1-\mu_u)^{\nu-d_H[S_j,S_k]}\mu_u^{d_H[S_j,S_k]} \quad (19)$$

where  $d_H[S_j, S_k]$  is the Hamming distance between the two sequences:

$$d_H[S_j, S_k] = \frac{1}{2} \left[ N - \sum_{l=1}^{\nu} s_j^l s_k^l \right]. \quad (20)$$

It is not difficult to see that the probabilities of erroneous replication become

$$W_{jk} = f(S_k)[\mu_u(1-\mu_u)]^{\nu/2} \exp\left(-K \sum_{l=1}^{\nu} S_j^l S_k^l\right) \quad (21)$$

where  $K = \log(\mu_u/(1-\mu_u))/2$ . This expression is identical to the transfer matrix for the two-dimensional Ising model [20,21,23]. Strictly, there are here two sources of noise associated to the model description. The previous spin-like description would be essentially valid at each phase separately. In this sense (and given the possibility that tumors might be close to the transition boundary) this system opens interesting problems for statistical physics: here two types of ‘‘particles’’ experience transitions with two different intrinsic temperatures.

Each generation in the algorithm we repeat  $N$  times the following set of rules:

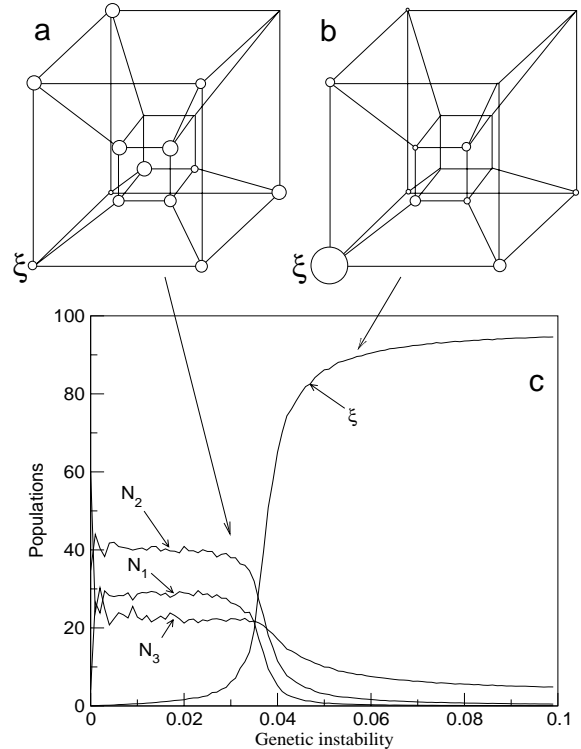


**Fig. 4.** Phase transition in the bit string quasispecies model involving genomes with small size  $\nu = 4$ . The dynamics takes place of a 4-dimensional hypercube (a-b) and the relative population size is indicated by means of the radius of the circles. In (c) the frequencies of strings  $N_i$  (differing  $i$  bits from the  $\xi$ -sequence) are shown against the instability level  $\mu_u$ . Here  $\mu = 0.01$ ,  $N = 10^2$ ,  $\alpha = 2$ ,  $f_1 = 0.25$  and  $\mu_u^* = 0.05$ . The mean field critical instability level, as predicted from equation (9) is  $\mu_u^c = 0.035$ .

1. we take a string at random from the population, say  $S_i$  and replicate it with probability  $f(S_i)$ .
2. Replication takes place by replacing one of the strings in the population (also chosen at random) say  $S_j \neq S_i$  by a copy of  $S_i$ . The copy mechanisms presents error, at rates  $\mu$  ( $x_1$  clone) and  $\mu_u$  (unstable population), per bit and replication cycle, respectively.

In Figure 4 we illustrate the transition occurring in the model for a small genome length  $\nu = 4$ . The four dimensional hypercube is shown in Figure 4a and 4b for  $\mu_u < \mu_u^c$  and  $\mu_u > \mu_u^c$ , respectively. Specifically, the number of strings  $N_i$  differing  $i$  bits from the  $\xi$ -sequence, *i.e.*

$$N_i = \sum_k^N \delta_{d_H[\xi,S_k],i} \quad (22)$$

are represented. Here string populations at each node in the hypercube are indicated by means of circles of different sizes. For  $\mu_u < \mu_u^c$ , given the higher replication rate of the unstable cells in relation with the  $\xi$  sequence, we have a population of genomes that occupy different zones of sequence space. Given the homogeneous character of

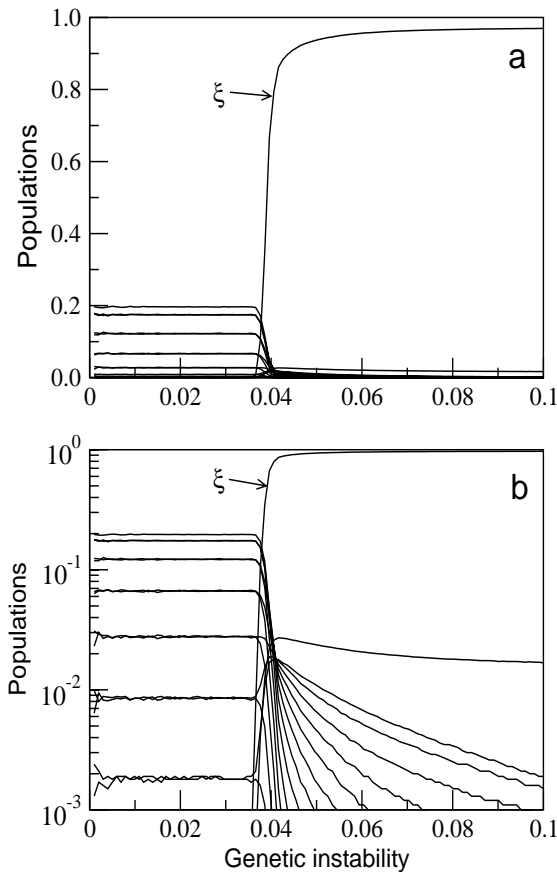


**Fig. 5.** Phase transition in the bit string quasispecies model (here linear (a) and linear-log (b) plots have been used). The population size is  $N = 500$  and the strings have length  $\nu = 16$  (averaged over  $10^2$  replicas). Frequencies are calculated over  $T = 500$  generations after  $\tau = 5000$  generations are discarded. A transition occurs at  $\mu_u \approx 0.036$ , where the master sequence experiences a sharp population increase once the critical instability level has been reached.

replication rates of the unstable clone, the sum of all sequences differing  $k$  bits from the master  $\xi$  will be  $\binom{\nu}{m}$  with a maximum at  $k = \nu/2$ . The probability distribution is thus a binomial, *i.e.*  $P_k = \binom{\nu}{m}(1 - \mu_u)^m \mu_u^{\nu-m}$ . In Figure 4c the population abundances of the  $\xi$ -sequence and those sequences with a Hamming distance  $d_H = i$  from it (here indicated as  $N_i$ ) are shown.

The sharpened character of the transition is clearly illustrated in Figure 5a–b. Here a  $\nu = 16$  genome has been used, with  $\mu = 10^{-3}$ . A transition is shown to occur at  $\mu_u^c \approx 0.037$ . We can compare this picture with the standard plots of quasispecies abundance against single-digit accuracy [14, 16]. In spite that the chain is not very long, a transition from the genetically unstable phase to the  $\xi$ -phase is clearly visible. Increasing genome lengths further increase the sharpening, with a wider domain of the  $\xi$  sequence. The time evolution of the  $\xi$ -sequence population is shown in Figure 6a–c for three different levels of instability close to criticality. Very close to the critical boundary (a–b) wild fluctuations are observed.

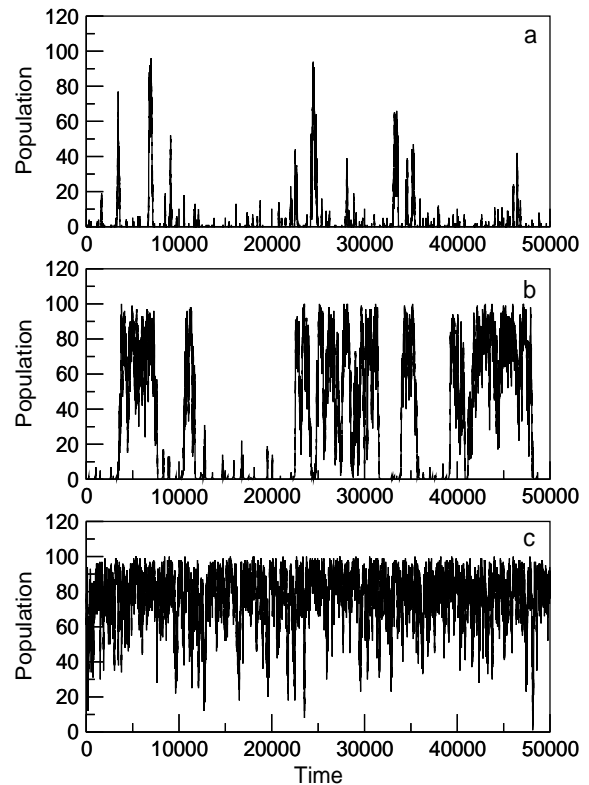


**Fig. 6.** Examples of the time evolution of the number of  $\xi$  strings close to the transition point. Here three situations are shown: (a) critical  $\mu_u \approx \mu_u^c = 0.036$  (b)  $\mu_u = 0.04 > \mu_u^c$ , where the master sequence starts to be dominant, but still highly fluctuations and (c)  $\mu_u = 0.042 > \mu_u^c$ , where most strings are  $\xi$ -type. Here we have  $N = 10^2$ ,  $\mu = 10^{-3}$ ,  $\nu = 16$ ,  $f_1 = 0.25$  and  $\alpha = 2.0$ .

Once we slightly increase the instability the  $\xi$  sequences dominate (c).

An additional statistical characterization of the genome population can be obtained by looking at the frequency distribution of  $\xi$  genomes at different mutation levels. Given the neutrality of  $S_i \in \mathcal{H}^\nu - \xi$  and the large size of sequence space (typically  $|\mathcal{H}^\nu| \gg N$ ) we take a mean field approximation in which mutations occur among cells in the unstable compartment at a rate  $\mu_u$  in such a way that any genome  $S_i \in \mathcal{H}^\nu - \xi$  can be introduced in the population as a consequence of mutation. In this way we completely ignore the correlations imposed by the mutation matrix. This situation is actually very close to the one considered in neutral models of biodiversity dynamics [30–32] where a finite, but large number of species  $S$  (here  $S \approx 2^\nu$ ) can be present in a finite urn of size  $N$ . The individuals behave as balls in a Polya process and replace each other at each generation with identical probabilities. Additionally, “mutations” are used in such a way that a different species from the  $S$ -pool is introduced through immigration at a rate  $\mu$ . In our system, immigration is replaced by true mutation (here at a rate  $\mu_u$ ).

By considering the previous partition into two basic sets, *i.e.*  $\xi$  and  $\mathcal{H}^\nu - \xi$  and indicating as  $P(n, t)$  the probability of finding a  $\xi$ -sequence represented by  $n$  strings, the

master sequence for the time evolution of this distribution will be [33]:

$$\frac{dP(n,t)}{dt} = r_{n+1}P(n+1,t) + g_{n-1}P(n-1,t) - (r_n + g_n)P(n,t) \quad (23)$$

where  $r_n = w(n-1|n)$  and  $g_n = w(n+1|n)$  are the transition probabilities associated to the one-step process described by the previous rules.

It is not difficult to compute the transition probabilities to be considered. First, we have

$$w(n-1|n) = P(n)f(\xi)\mu^* \frac{n}{N} \left(1 - \frac{n-1}{N-1}\right) + P(n)\alpha f(\xi)\phi(\mu_u) \left[1 - \frac{1}{2^\nu - 1}\right] \frac{n}{N} \left(1 - \frac{n-1}{N-1}\right) \quad (24)$$

where two basic terms have been introduced. The first term in the right-hand side is the contribution to the  $n \rightarrow n-1$  transition due to incorrect replication of the  $\xi$  sequence. The probability of wrong replication is indicated as  $\mu^* = 1 - (1-\mu)^\nu$ . The second term corresponds to replication of a  $S_k \neq \xi$  sequence that is replicated at the expense of a  $\xi$  copy. The term  $1 - 1/(2^\nu - 1)$  indicates that the replication event must generate another sequence  $S_j \neq \xi$ . Given the assumed large size of sequence space, this term will be very close to one.

Similarly, it can be shown that

$$w(n-1|n) = P(n)f(\xi)(1-\mu)^\nu \frac{n}{N} \left(1 - \frac{n-1}{N-1}\right). \quad (25)$$

Assuming that  $\mu \ll 1$ , we have the approximate transition probabilities

$$r_n = P(n)f(\xi) \frac{n}{N} \left(1 - \frac{n-1}{N-1}\right) (1 + \alpha\phi(\mu_u)) \quad (26)$$

$$g_n = P(n)f(\xi) \frac{n}{N} \left(1 - \frac{n-1}{N-1}\right). \quad (27)$$

A further constraint can be introduced if we consider that the population is in the  $\mu_u \approx \mu_u^c$  boundary and thus  $x = n/N$  is small. The continuous limit of the master equation gives [34]:

$$\frac{\partial P(x,t)}{\partial t} = f(\xi)\phi(\mu_u^c) \frac{\partial}{\partial x} xP(x,t) + \frac{1}{2} f(\xi)(2 + \alpha\phi(\mu_u^c)) \frac{\partial^2}{\partial x^2} xP(x,t) \quad (28)$$

with a stationary solution

$$P^*(x) \sim x^{-1} \exp(-\Phi(\mu_u^c)x) \quad (29)$$

with  $\Phi(\mu_u^c) = \phi(\mu_u^c)/(2 + \alpha\phi(\mu_u^c))$ . For  $\mu_u \rightarrow \mu_u^c$ , the cut-off will be large and a scaling law  $P^*(n) \sim n^{-1}$  will be observed. This prediction is illustrated in Figure 7, where the distribution of  $\xi$ -genomes for a  $N = 10^2$  population with  $\nu = 16$  is shown at the  $\mu_u \approx \mu_u^c$  transition (open circles). Once we move far from the phase transition point (open circles) the scaling law is quickly replaced by a single-maximum distribution (filled triangles).

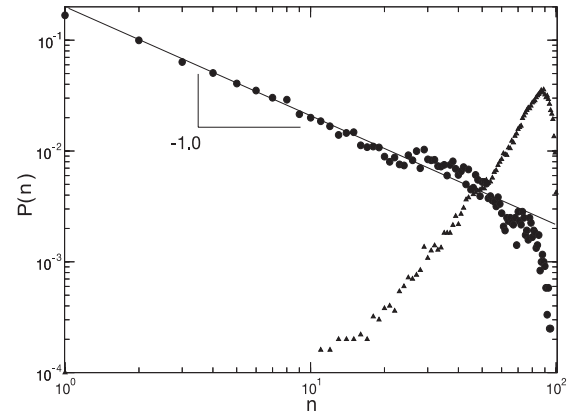


**Fig. 7.** Probability distributions associated to the master sequence  $\xi$  for (a) the critical region  $\mu_u \approx \mu_u^c = 0.036$  (open circles) and for (b)  $\mu_u = 0.042 > \mu_u^c$  (filled triangles). Here we have  $N = 10^2$ ,  $\mu = 10^{-3}$ ,  $\nu = 16$ ,  $f_1 = 0.25$  and  $\alpha = 2.0$ . At criticality we have a scaling behavior  $P(n) \sim n^{-1}$ , as predicted by the master equation approach. Once the level of genetic instability is slightly increased, the master sequence starts to dominate and thus a single peak is obtained.

## 4 Discussion

One particular difference in relation with the standard problems considered by quasispecies models concerns the way genetic instability emerges in cancer cells. In RNA viruses, mutation rates are tuned through evolution in order to reach the error threshold. In this way, the greatest adaptability emerges close to the order-disorder boundary defined by the error catastrophe [17].

For unstable tumors, the situation is somewhat different: here we have genes that are involved in preserving genome integrity that are mutated or simply removed from the genome (through gene or chromosome loss). As a consequence, the molecular machinery implicated in maintaining a correct cellular functioning is absent and mutations accumulate at high levels. Genetic instability is thus an intrinsic feature of the unstable cell that is carried out through tumor progression [10]. Different levels of genetic instability are likely to be present within the population and those cells with too high levels will probably die out. Since the critical mutation rates defined by the quasispecies model scale with genome length as  $\mu_c \sim \nu^{-1}$ , we should expect to observe supercritical mutation levels at least at early tumor progression. Afterwards, it should stabilize close to the critical instability. However, it is important to mention one possible scenario emerging from this model approach: if instability levels keep increasing, the tumor might actually become too unstable and *tumor regression would eventually occur*. This situation should be explored within the context of cancer regression.

Strictly speaking, tumor progression is a coevolution process in which cancer population responses are modulated by the host response. In this sense, further work should consider this host-tumor interaction, which eventually might tune mutation and replication rates, as it seems to be the case with RNA viruses [3,4,6,35].

The present model is an oversimplified picture of cancer cells populations. Even for RNA viruses the assumption of a single-peak fitness function is a very strong one, and experimental evidence shows that the structure of the landscape is case-dependent [36,37]. Genome sizes are very small and a more appropriate representation would be to consider the  $S_i$ 's as genes themselves. In that case, the tumor population would evolve through adaptive walks performed by cells through gene space [38]. Additionally, the previous analysis is performed under the assumption of stationarity, *i.e.* a maximum cell population size is allowed and competition takes place under this population constraint. Real tumors are nonequilibrium systems and as such are growing structures. Besides, spatial degrees of freedom seem to be relevant in maintaining and propagating genetic heterogeneity in such a way that competition among different clones is effectively reduced under the local character of cell-cell interactions [39]. Finally, the evolution of the cell population towards the instability boundary should be introduced in an explicit way, by allowing replication and mutation rates to be self-tuned. In spite of these drawbacks, current research seems to indicate that the previous results are robust (R.V. Solé, unpublished).

If there is such an error threshold in unstable cancer populations, perhaps we could take advantage of treatments in which the tumor cells are destabilized by means appropriate drugs. This possibility has been suggested by some authors [10,12,26] provided that the tumors operate close to instability thresholds. The current model strongly supports the idea that such thresholds exist and indicates that cell population responses close to such threshold are expected to be sharp.

The author thanks Isabel González, Thomas Deisboeck and Josep Costa for useful discussions. This work was supported by a grant BFM2001-2154 and by the Santa Fe Institute.

## References

1. G.R. Andersson, D.L. Stoler, B.M. Brenner, *Bioessays* **23**, 1037 (2001)
2. G. Weisbuch, A. Perelson, *Rev. Mod. Phys.* **69**, 1219 (1997)
3. C. Kamp, S. Bornholdt, *Phys. Rev. Lett.* **88**, 068104 (2002)
4. C. Kamp, C.O. Wilke, C. Adami, S. Bornholdt, *Complexity* **8**(2), 28 (2003)
5. C. Kamp, S. Bornholdt, *Proc. Roy. Soc. London B* **269**, 2035 (2002)
6. S. Bonhoeffer, P. Sniegowski, *Nature* **420**, 367 (2002)
7. B. Alberts, A. Johnson, J. Lewis, M. Raff, K. Roberts, P. Walter *Molecular Biology of the Cell*, 4th edn. (Garland, New York, 2002)
8. J.H.J. Hoeijmakers, *Nature* **411**, 366 (2001)
9. A.L. Jackson, L.A. Loeb, *Genetics* **148**, 1483 (1998)
10. D.P. Cahill, K.W. Kinzler, B. Vogelstein, C. Lengauer, *Trends Genet.* **15**, M57 (1999)
11. C. Lengauer, K.W. Kinzler, B. Vogelstein, *Nature* **396**, 643 (1998)
12. L.A. Loeb, K.R. Loeb, J.P. Anderson, *Proc. Natl. Acad. Sci. USA* **100**, 776 (2003)
13. F. Michor, Y. Iwasa, N.L. Komarova, M.A. Nowak, *Curr. Biol.* **13**, 581 (2003)
14. J. Swetina, P. Schuster, *Biophys. Chem.* **16**, 329 (1982)
15. M. Eigen, *Naturwiss.* **58**, 465 (1971)
16. M. Eigen, J. McCaskill, P. Schuster, *Adv. Chem. Phys.* **75**, 149 (1987)
17. P. Schuster, in: *Complexity: metaphors, models and reality*, edited by G.A. Cowan, D. Pines, D. Meltzer (Addison-Wesley, Reading, MA, 1994), pp. 383-418
18. L. Peliti, *Europhys. Lett.* **57**, 745 (2002)
19. E. Domingo, *Virology* **270**, 251 (2000)
20. I. Leuthäusser, *J. Chem. Phys.* **84**, 1884 (1986)
21. I. Leuthäusser, *J. Stat. Phys.* **48**, 343 (1987)
22. D. Alves, J.F. Fontanari, *Phys. Rev. E* **54**, 4048 (1996)
23. P. Tarazona, *Phys. Rev. A* **45**, 6038 (1992)
24. R. Pastor-Satorras, R.V. Solé, *Phys. Rev. E* **64**, 051909 (2002)
25. L.A. Loeb, J.M. Essigmann, F. Kazazi, J. Zhang, K.D. Rose, J.I. Mullins, *Proc. Natl. Acad. Sci. USA* **96**, 1492 (1999)
26. R.V. Solé, T.S. Deisboeck, SFI working paper 03-02-002
27. C. Adami, *Artificial Life* (Springer, New York, 1998)
28. W. Fontana, W. Schnabl, P. Schuster, *Phys. Rev. A* **40**, 3301 (1989)
29. R.V. Solé, R. Ferrer, I. Gonzalez-Garcia, J. Quer, E. Domingo *J. Theor. Biol.* **198**, 47 (1999)
30. R.V. Solé, D. Alonso, *Adv. Complex Syst.* **1**, 203 (1998)
31. R.V. Solé, D. Alonso, A. McKane, *Physica A* **286**, 337 (2000)
32. A. McKane, D. Alonso, R.V. Solé, *Phys. Rev. E* **62**, 8466 (2000)
33. N.G. van Kampen, *Stochastic Processes in Physics and Chemistry* (Elsevier, Amsterdam, 1981)
34. D.J. Bicout, M.J. Field, *Phys. Rev. E* **54**, 726 (1996)
35. M. Nowak, R.M. May, *Virus Dynamics* (Oxford U. Press, Oxford, 2000)
36. A. Grande-Perez, S. Sierra, M.G. Castro, E. Domingo, P.R. Lowenstein, *Proc. Natl. Acad. Sci. USA* **99**, 12938 (2002)
37. M. Eigen, *Proc. Natl. Acad. Sci. USA* **99**, 13374 (2002)
38. S.A. Kauffman, *The Origins of Order* (Oxford, New York, 1993)
39. I. González-García, R.V. Solé, J. Costa, *Proc. Natl. Acad. Sci. USA* **99**, 13085 (2002)